

# Providing Active Charging Services: An Assignment Strategy with Profit-Maximizing Heat Maps for Idle Mobile Charging Stations

Linfeng Liu, *Member, IEEE*, Houqian Zhang, Jia Xu, *Senior Member, IEEE*, and Ping Wang, *Fellow, IEEE*

**Abstract**—In Internet of Electric Vehicles (IoEV), mobile charging stations (MCSs) have been deployed to complement fixed charging stations. Typically, MCSs are assigned to charge the electric vehicles with insufficient electricity which have made charging requests (termed IEVs). Moreover, there are some electric vehicles with insufficient electricity which have not made charging requests (termed quasi-IEVs). If idle MCSs are allowed to actively track quasi-IEVs according to their potential charging demand, then more IEVs could be promptly charged, and thus the charging profits of MCSs could be increased. However, due to the private ownership of electric vehicles, some private information cannot be provided in the potential charging demand of quasi-IEVs (e.g., the destinations and residual electricity), making the potential charging profits of idle MCSs hard to be evaluated, and thereby the proper assignments of idle MCSs are difficult to decide. To this end, we introduce the profit-maximizing heat maps to depict the potential charging demand of quasi-IEVs and evaluate the potential charging profits of idle MCSs. A profit-maximizing heat map remarks the positions around quasi-IEVs and displays them as continuous areas. Specifically, the different shades of colours are used to distinguish the quantities of potential charging profits of idle MCSs, and the sizes of coloured areas are used to indicate the possibility of quasi-IEVs passing through these positions. In this paper, we propose a Profit-Maximizing Assignment Strategy of Idle MCSs (PMASIM) to properly assign the idle MCSs to charge IEVs at selected charging positions, or track some quasi-IEVs according to the profit-maximizing heat maps. Extensive simulations and comparisons demonstrate the superior performance of PMASIM, i.e., with the profit-maximizing heat maps, the charging profits of MCSs are increased, and the proportion of charged IEVs is enhanced as well.

**Index Terms**—Internet of Electric Vehicles; mobile charging station; profit-maximizing heat map; MCS assignment.

## I. INTRODUCTION

Recently, the number of electric vehicles (EVs) in the transportation network is increased quickly, due to the increasing concern on greenhouse gas emission [1], [2]. Internet of Electric Vehicles (IoEV) [3] is mainly constituted by EVs and charging facilities.

The battery condition of EVs is quite sensitive to external environment (such as the air temperature), and the mileage

L. Liu, H. Zhang, and J. Xu are with the Jiangsu Key Laboratory of Big Data Security and Intelligent Processing, Nanjing University of Posts and Telecommunications, China ({liulf,xujia}@njupt.edu.cn, houqianzhang@163.com).

P. Wang is with the Department of Electrical Engineering and Computer Science, York University, Canada (email: pingw@yorku.ca).

endurance of EVs is not stable as gasoline vehicles. Thus, the "mileage anxiety" of EVs is much more serious than that of gasoline vehicles, especially in the zones where fixed charging stations (FCSs) are sparsely deployed or absent. To provide active charging services for EVs, mobile charging stations (MCSs) [4], [5] (Fig. 1) have been introduced as an alternative charging solution [6]. At present, there are two strategies for the usage of MCSs: (i) The main strategy of MCSs is to remain stationary and move towards EVs only after being requested, i.e., MCSs move to charge EVs only when they have received the charging requests; (ii) MCSs also play the role of "movable FCSs", e.g., MCSs could move into some hotspots on holidays to provide charging services, and they do not move after being deployed until the end of holidays.

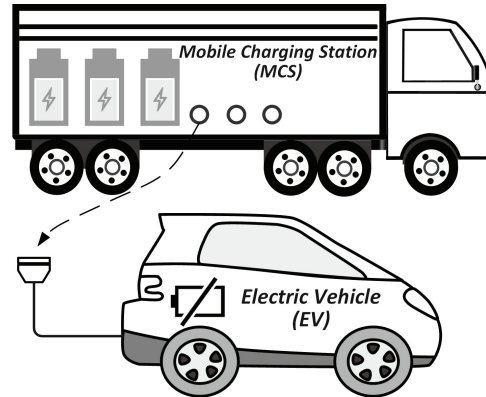


Fig. 1: An MCS charges an EV.

Some EVs do not have sufficient electricity to sustain the travels to their destinations. An EV with insufficient electricity could make a charging request to the cloud server for the mobile charging service. Upon receiving the charging request, the cloud server assigns an MCS to charge the EV. In this paper, an EV with insufficient electricity which has made a charging request to the cloud server is referred to as an IEV, and an EV with insufficient electricity which has not made a charging request is referred to as a quasi-IEV. Apparently, quasi-IEVs must be charged in future, although they have not made the charging requests. However, the time points of quasi-IEVs making charging requests are difficult to predict, due to the different charging considerations and charging habits of their drivers. For example, some drivers are prone to make quasi-IEVs charged

earlier (when quasi-IEVs are with more residual battery electricity), while other drivers are prone to make quasi-IEVs charged when there is less residual battery electricity because they think they could encounter some FCSs along the routes to the destinations (the charging price of FCSs is lower than that of MCSs).

Naturally, the charging profits of MCSs (the profits earned by charging IEVs) could be increased if idle MCSs are allowed to actively track some quasi-IEVs, since more quasi-IEVs can be promptly charged in future when idle MCSs actively move close to some quasi-IEVs. An example is given in Fig. 2 with an idle MCS and a quasi-IEV. The idle MCS actively moves close to the quasi-IEV, and thus the quasi-IEV is likely to be charged by the MCS once it makes a charging request and turns into an IEV. Accordingly, the charging profit of this MCS is increased.

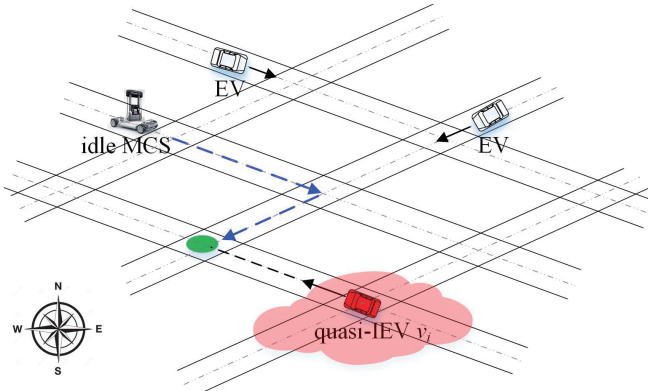


Fig. 2: An idle MCS is assigned to track a quasi-IEV.

The proper assignments of idle MCSs can increase the charging profits of MCSs and enhance the proportion of charged IEVs. In this paper, we investigate the assignments of idle MCSs in the following two cases:

*Case A.* Assignments of idle MCSs for IEVs. The cloud server assigns idle MCSs to charge IEVs at the selected positions.

*Case B.* Assignments of idle MCSs for quasi-IEVs. Typically, MCSs are sparsely distributed on a road lattice, and many quasi-IEVs could not be charged within an allowable extra delay after they turn into IEVs, because they may be far away from MCSs. Thus, the cloud server could assign idle MCSs to move towards the tracking positions of some quasi-IEVs (i.e., idle MCSs actively track some quasi-IEVs) for the potential charging in future. The tracking positions of quasi-IEVs are selected from the available charging positions provided and updated by the quasi-IEVs.

In Case B, quasi-IEVs periodically determine and upload their potential charging demand including the insufficient electricity and the tracking positions. Note that the privacy protection is a vital issue for EVs, and some private information regarding EVs (e.g., the destinations and the residual electricity<sup>1</sup>) should not be uploaded to the cloud

<sup>1</sup>Because the private travel intention of a quasi-IEV is revealed by the destination information, and the possible scope of destination can be inferred from the residual electricity.

server. Lack of these private information, the cloud server is hard to measure the possibility of quasi-IEVs passing through the tracking positions in future, especially when the road segments have extremely different lengths and/or shapes. Thereby, the potential charging profits of idle MCSs are hard to be evaluated.

An example is illustrated in Fig. 3 with a quasi-IEV and ten tracking positions. The destination information of the quasi-IEV is not uploaded to the cloud server, and hence the cloud server cannot foreknow that the quasi-IEV will move towards *Area 1* or *Area 2*, and how far it will move before making a charging request, which implies that the future charging position cannot be predicted. Accordingly, the potential charging profit obtained by an MCS for charging this quasi-IEV cannot be evaluated. Suppose the quasi-IEV moves towards *Area 1*, an idle MCS could move towards *Area 1* (track the quasi-IEV) for earning a charging profit from the quasi-IEV.

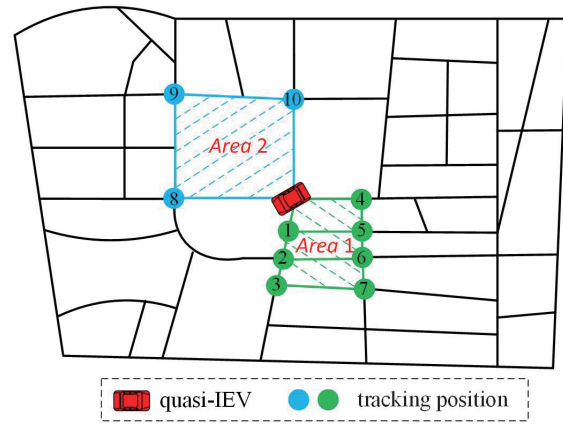


Fig. 3: Future movement of a quasi-IEV.

To this end, the concept of heat maps [7], [8] is applied to depict the potential charging demand of quasi-IEVs. A heat map is a graphical representation of data where the individual values contained in a matrix are represented as colours. In our proposed Profit-Maximizing Assignment Strategy of Idle MCSs (PMASIM), the profit-maximizing heat maps remark the tracking positions of quasi-IEVs and display them as continuous areas. In the profit-maximizing heat maps, different shades of colours are used to distinguish the quantities of potential charging profits of idle MCSs, and the sizes of coloured areas are used to indicate the possibility of quasi-IEVs passing through the tracking positions. Thus, idle MCSs are assigned to charge IEVs at selected charging positions, or move towards the tracking positions of quasi-IEVs by the profit-maximizing heat maps.

As shown in Fig. 4, in PMASIM, when the cloud server receives the charging requests from IEVs, it selects the optimal idle MCSs and charging positions on the basis of the objective of charging profit maximization, and then assigns these idle MCSs to charge IEVs at the selected charging positions. Furthermore, the cloud server evaluates the potential charging profits of tracking quasi-IEVs by the profit-maximizing heat maps, and assigns idle MCSs to

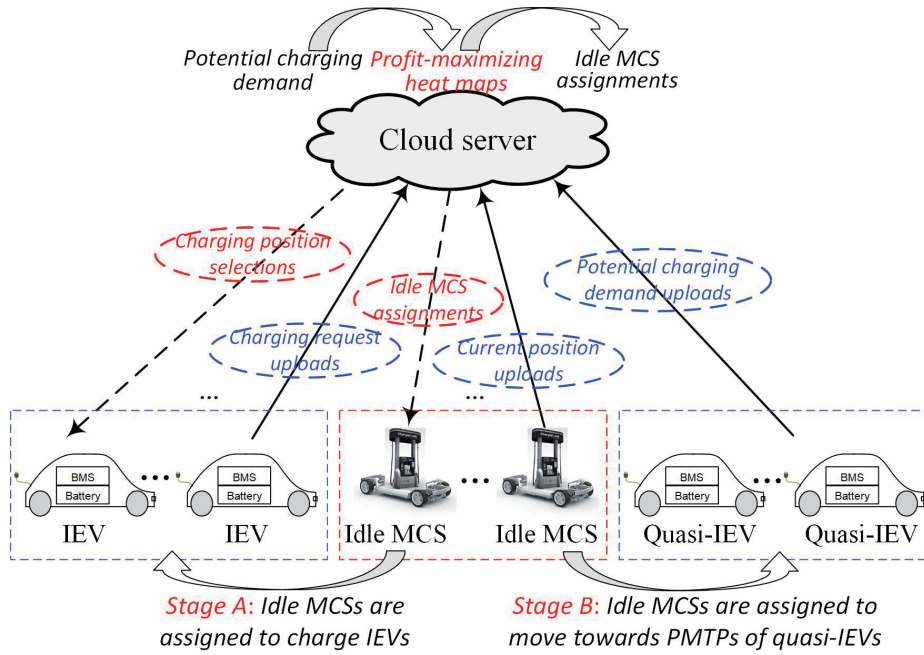


Fig. 4: A framework for assignments of idle MCSs.

move towards the Profit-Maximization Tracking Positions (PMTPs) of some quasi-IEVs for the potential charging in future. Especially, the overlapped areas in profit-maximizing heat maps are observed, and an idle MCS can move towards a PMTP shared by several quasi-IEVs. Such mechanism can further reduce the charging cost of MCSs and increase their charging profits.

The remainder of this paper is organized as follows: Section II surveys some related works. Section III formulates the problem of MCS assignments. Section IV proposes the Profit-Maximization Assignment Strategy of Idle MCSs (PMASIM). Section V provides some analyses on PMASIM, in terms of complexity and expected charging profit of an MCS. Section VI presents some simulation results to evaluate the performance of PMASIM. Section VII concludes this paper.

## II. RELATED WORK

### A. Charging with Fixed Charging Stations

As a major charging solution, FCSs have been deployed in many cities to provide the charging services for EVs, and some related research has investigated the optimal charging routes of EVs and the optimal layout of FCSs. In [9], a VANET-enhanced charging strategy is developed to reduce the energy consumption and travel cost of EVs while averting the overload of power system. Likewise, [10] attempts to optimize the route selections and charging/discharging schedules to minimize the total cost of all EVs, and the  $A^*$  algorithm is adopted to find the  $K$ -shortest route paths for EVs.

However, the mobility of charging stations is not considered in most of the related works regarding FCSs.

### B. Charging with Mobile Charging Stations

Some relevant research has been conducted on the problem of MCS assignments. For example, a Lyapunov-based optimization algorithm is presented in [5] to increase the business profits of MCSs, through deciding the optimal strategy of power management. In [11], a framework is designed for assigning MCSs to charge EVs according to the charging demand of EVs. Besides, an optimization problem is introduced in [12] to minimize the charging cost while satisfying the movement constraints of MCSs and the deadline constraints of charging requests, and a method of modified Clarke and Wright Saving's heuristics is proposed to solve this problem.

[6] provides a reservation-based approach (RBA) based on the context collected from the charging network, and readily available MCSs can be predicted and scheduled toward EVs with charging demand. In [13], the route scheduling problem of EVs is formulated to maximize the total residual electricity of EVs and make all EVs can reach their destinations before deadlines. Our early works [14], [15] investigate the problem of MCS assignments. In [14], the assignments of MCSs are decided according to the charging requests of IEVs, and these assignments can be dynamically rescheduled with the time-variant charging demand of IEVs. Specially, the assignments of idle MCSs for potential charging demand are not considered in [14]. Besides, [15] decides the assignments of idle MCSs by learning the historical routes and charging records of MCSs, and the information of EVs does not need to be provided to MCSs.

In the above works, the potential charging demand of quasi-IEVs is not taken into account, and the potential charging demand is hard to be estimated, especially when

some private information regarding quasi-IEVs is not retrievable.

### C. Heat Maps and Applications

In some previous works, the heat maps have been exploited to visualize some data sets or events, such as [16], [17], where the heat maps are taken to reflect the population density in some hot spots, and thus the maximum air-conditioning load can be estimated. In [18], the traffic accident data of Olomouc city is visualized by changing the color range, kernel size, radius, and transparency of the heat maps.

Heat maps can depict the interaction of heterogenic data at different levels over time. To the best of our knowledge, the heat maps have not been applied to depict the potential charging demand of quasi-IEVs. In our work, the profit-maximizing heat maps concerning the potential charging demand of quasi-IEVs are generated: The different shades of colours are used to distinguish the quantities of potential charging profits of idle MCSs, and the sizes of coloured areas are used to indicate the possibility of quasi-IEVs passing through positions. The profit-maximizing heat maps conceal the private information of quasi-IEVs, and the potential charging demand uploaded to the cloud server does not contain the destinations and residual electricity of quasi-IEVs. Based on the profit-maximizing heat maps, the cloud server can determine the PMTPs of quasi-IEVs and assign some idle MCSs to move towards these PMTPs.

## III. SYSTEM MODEL AND PROBLEM FORMULATION

The road lattice in the 2D plane is denoted by  $\mathcal{R}$ . The sets of road segments and road intersections are denoted by  $\mathcal{S}$  and  $\mathcal{I}$ , respectively. The road segments could have different lengths and/or different forms. The charging positions and tracking positions are selected from  $\mathcal{I}$ .

The charging scenario occurs in the zones where FCSs are sparsely deployed or absent, and some MCSs are deployed to provide the charging services for IEVs. Several charging parks could be set up for MCSs charging IEVs, which can be taken as a special case of this system model where MCSs can charge IEVs at any road intersections. Time is divided into discrete time slots with an equal length of  $t_s$ . TABLE I shows the list of main notations.

### A. Mobile Charging Stations and Electric Vehicles

There are  $M$  MCSs, and the set of MCSs is denoted by  $\mathcal{M}$ . For an MCS  $\psi_j$  which is assigned to charge one or more IEVs at the  $t$ -th time slot, the selected charging position of  $\psi_j$  is labeled by  $p_c(\psi_j)^{(t)}$ , where  $p_c(\psi_j)^{(t)} \in \mathcal{I}$ . An MCS which is not assigned to charge any IEVs is referred to as an idle MCS.

There are  $N$  EVs, and the set of EVs is denoted by  $\mathcal{E}$ . The departure position and the destination of an EV  $v_i$  are denoted by  $s_i$  and  $d_i$ , respectively, where  $s_i, d_i \in \mathcal{I}$ .  $v_i$  moves at a speed of  $m_s(v_i)$ , and  $c$  units of electricity are consumed for moving through a unit distance.

TABLE I: Main notations

Parameter	Description
$\mathcal{R}$	Road lattice
$\mathcal{I}$	Set of road intersections
$\mathcal{S}$	Set of road segments
$\mathcal{E}$	Set of EVs
$\mathcal{M}$	Set of MCSs
$m_s(v_i)$	Moving speed of EV $v_i$
$e(v_i)^{(t)}$	Residual electricity of EV $v_i$ at the $t$ -th time slot
$e(v_i)^{(0)}$	Battery capacity of EV $v_i$
$p(v_i)^{(t)}$	Current position of EV $v_i$ at the $t$ -th time slot
$p(\psi_j)^{(t)}$	Current position of MCS $\psi_j$ at the $t$ -th time slot
$p_c(\psi_j)^{(t)}$	Charging position of MCS $\psi_j$ at the $t$ -th time slot
$E_m(v_i, \tilde{p})$	Extra movement of EV $v_i$ being charged at the position $\tilde{p}$
$E_m(\psi_j)^{(t)}$	Movement distance of MCS $\psi_j$ if $\psi_j$ is in the idle state at the $t$ -th time slot
$\mathcal{V}(\psi_j, \tilde{p})$	Set of IEVs to be charged by MCS $\psi_j$ at the position $\tilde{p}$
$t_w(v_i, \psi_j, \tilde{p})$	Time of EV $v_i$ waiting for MCS $\psi_j$ at the position $\tilde{p}$
$\bar{D}$	Allowable extra delay
$\xi$	Charging power of MCSs
$delay(v_i, \psi_j, \tilde{p})$	Extra delay of EV $v_i$ after being charged by MCS $\psi_j$ at the position $\tilde{p}$
$Exp(v_i, \psi_j, \tilde{p})$	Charging expense of EV $v_i$ paid to MCS $\psi_j$
$Profit(\psi_j)$	Charging profit of MCS $\psi_j$
$r_e$	Unit price of electricity transferred from MCSs to IEVs
$r_0$	Unit price of electricity purchased from power grid

Suppose an EV  $v_i$  does not have sufficient electricity to move from  $s_i$  to  $d_i$  (i.e.,  $e(v_i)^{(0)} < c \cdot |s_i - d_i|$ , where  $|s_i - d_i|$  denotes the travel distance from  $s_i$  to  $d_i$ ), and then  $v_i$  is taken as a quasi-IEV. When  $v_i$  detects a low battery state (e.g.,  $e(v_i)^{(t)} \leq \frac{e(v_i)^{(0)}}{\gamma}$  at the  $t$ -th time slot), or makes a charging request to the cloud server before the low battery state, then  $v_i$  is taken as an IEV.

### B. Charging Model for MCSs and IEVs

When an MCS  $\psi_j$  is assigned to charge an IEV  $v_i$  at the selected charging position  $\tilde{p}$  at the  $t$ -th time slot, the extra movement (the distance deviation from the destination) undertaken by  $v_i$  is written as [15]:

$$E_m(v_i, \tilde{p}) = |p(v_i)^{(t)} - \tilde{p}| + |\tilde{p} - d_i| - |p(v_i)^{(t)} - d_i|, \quad (1)$$

where  $|p(v_i)^{(t)} - \tilde{p}| + |\tilde{p} - d_i|$  denotes the travel distance of future movement of  $v_i$  passing through the charging position  $\tilde{p}$ , as illustrated in Fig. 5.

Note that the road segments could be with different forms and lengths, which does not affect the assignment decisions in our proposed strategy, because the travel distance of MCSs and EVs is independent of the forms and lengths of road segments. Thus, our proposed strategy can be applied in different road networks.

When  $\psi_j$  charges  $v_i$ , the amount of electricity transferred from  $\psi_j$  to  $v_i$  is expressed as:

$$\begin{aligned} \Delta e(v_i, \tilde{p}) = \\ \min \left\{ c \cdot \{|s_i - d_i| + E_m(v_i, \tilde{p})\} - e(v_i)^{(0)}, e(v_i)^{(0)} \right\}, \end{aligned} \quad (2)$$

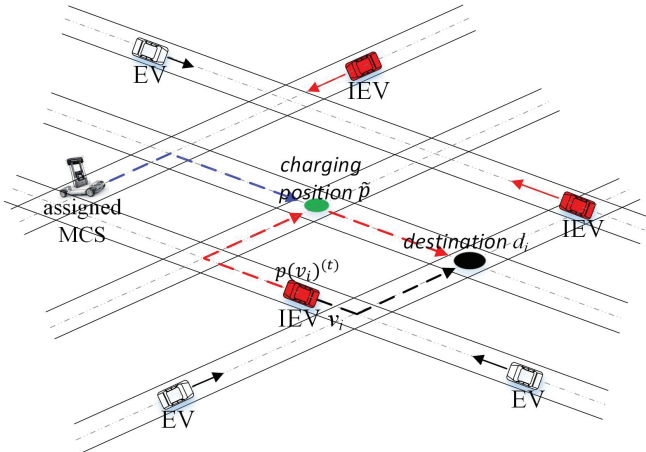


Fig. 5: Extra movement of an IEV.

where  $\Delta e(v_i, \tilde{p})$  is calculated as the insufficient electricity of  $v_i$  for supporting the future movement to the destination  $d_i$ . (2) indicates that an IEV only get the essential electricity from MCSs, due to the facts that the charging price of MCSs is larger than that of FCSs, and MCSs typically provide the emergent charging services.

When  $v_i$  takes a long-distance travel, there is  $c \cdot \{|s_i - d_i| + E_m(v_i, \tilde{p})\} - e(v_i)^{(0)} > e(v_i)^{(0)}$ , i.e.,  $\Delta e(v_i, \tilde{p}) = e(v_i)^{(0)}$ , and  $v_i$  should be charged by some MCSs several times.

Besides, the time of  $v_i$  waiting for  $\psi_j$  at the charging position  $\tilde{p}$  is calculated by:

$$t_w(v_i, \psi_j, \tilde{p}) = \begin{cases} 0, & \text{if } \frac{|p(v_i)^{(t)} - \tilde{p}|}{m_s(v_i)} \geq \frac{|p(\psi_j)^{(t)} - \tilde{p}|}{m_s(\psi_j)}, \\ \frac{|p(\psi_j)^{(t)} - \tilde{p}|}{m_s(\psi_j)} - \frac{|p(v_i)^{(t)} - \tilde{p}|}{m_s(v_i)}, & \text{otherwise.} \end{cases} \quad (3)$$

Then, the extra delay of  $v_i$  is expressed as:

$$\text{delay}(v_i, \psi_j, \tilde{p}) = \frac{E_m(v_i, \tilde{p})}{m_s(v_i)} + t_w(v_i, \psi_j, \tilde{p}) + \frac{\Delta e(v_i, \tilde{p})}{\xi}, \quad (4)$$

which indicates that the extra delay of  $v_i$  is comprised of three parts: the time consumed for the extra movement, the time of waiting for the assigned MCS, and the time of being charged by the assigned MCS.

The extra delay of each IEV should be restricted by an allowable extra delay  $\tilde{D}$  to guarantee the travel experience and prompt arrival. For an IEV  $v_i$  there must be  $\text{delay}(v_i, \psi_j, \tilde{p}) \leq \tilde{D}$ . The setting of allowable extra delay is related to the QoS requirements of EV drivers. A shorter allowable extra delay indicates more emergent travel intentions of EV drivers.

### C. Charging Expenses of IEVs and Charging Profits of MCSs

Suppose an IEV  $v_i$  makes a charging request to the cloud server, and an MCS  $\psi_j$  is assigned to charge several IEVs (including  $v_i$ ) at the charging position  $\tilde{p}$ . The charging expense of  $v_i$  paid to  $\psi_j$  is calculated by:

$$\text{Exp}(v_i, \psi_j, \tilde{p}) = r_e \cdot \Delta e(v_i, \tilde{p}), \quad (5)$$

where  $r_e$  denotes the unit price of electricity transferred from MCSs to IEVs. The charging profit obtained by  $\psi_j$  is expressed as:

$$\text{Profit}(\psi_j) = \begin{cases} -r_0 \cdot c \cdot E_m(\psi_j)^{(t)}, & \text{if } \psi_j \text{ is idle,} \\ \sum_{v_i \in \mathcal{V}(\psi_j, \tilde{p})} \{\text{Exp}(v_i, \psi_j, \tilde{p}) - r_0 \cdot \Delta e(v_i, \tilde{p})\} & \\ -r_0 \cdot c \cdot |p(\psi_j)^{(t)} - \tilde{p}|, & \text{otherwise,} \end{cases} \quad (6)$$

where  $E_m(\psi_j)^{(t)}$  denotes the movement distance of  $\psi_j$  if  $\psi_j$  is in the idle state at the  $t$ -th time slot.  $r_0$  denotes the unit price of electricity purchased by MCSs from power grid. If  $\psi_j$  has been assigned to charge IEVs,  $\mathcal{V}(\psi_j, \tilde{p})$  denotes the set of IEVs to be charged by  $\psi_j$  at the position  $\tilde{p}$ .

In (6),  $|p(\psi_j)^{(t)} - \tilde{p}|$  is the distance of  $\psi_j$  moving from current position to the charging position  $\tilde{p}$ . Thus,  $r_0 \cdot c \cdot E_m(\psi_j)^{(t)}$  and  $r_0 \cdot c \cdot |p(\psi_j)^{(t)} - \tilde{p}|$  denotes the charging cost of  $\psi_j$ .

### D. Objective Function

To maximize the charging profits of MCSs, the problem objective of MCS assignments is formally presented as follows:

$$\max_{\psi_j \in \mathcal{M}} \sum_{t=1}^T \text{Profit}(\psi_j), \quad (7)$$

where  $\sum_{t=1}^T \text{Profit}(\psi_j)$  denotes the cumulative charging profit of  $\psi_j$  during an observation period  $T \cdot t_s$  (such as a day or a week).

In the next section, we will propose a Profit-Maximizing Assignment Strategy of Idle MCSs (PMASIM) to properly assign the idle MCSs. In PMASIM, the idle MCSs are assigned to charge IEVs at the selected charging positions. Moreover, some idle MCSs are assigned to actively move towards the PMTPs of some quasi-IEVs to track them, through generating and exploiting the profit-maximizing heat maps. Therefore, more IEVs can be promptly charged, and the charging profits of MCSs can be increased.

In essence, the objective of charging profit maximization enables MCSs to spend as much time as possible on charging IEVs and reduce their charging cost, which can enhance the charging efficiency of MCSs and the proportion of charged IEVs.

## IV. HEAT MAP BASED ASSIGNMENT STRATEGY OF IDLE MCSs

There are two cases for the assignments of idle MCSs: the assignments of idle MCSs for IEVs, and the assignments of idle MCSs for quasi-IEVs. In this section, we provide the detailed stages of PMASIM, as depicted in Fig. 6. Specially, at each time slot *Stage A* is executed before *Stage B*, i.e., the idle MCSs are preferentially assigned to charge IEVs rather than to track quasi-IEVs, and this arrangement will be demonstrated in Section V.B.

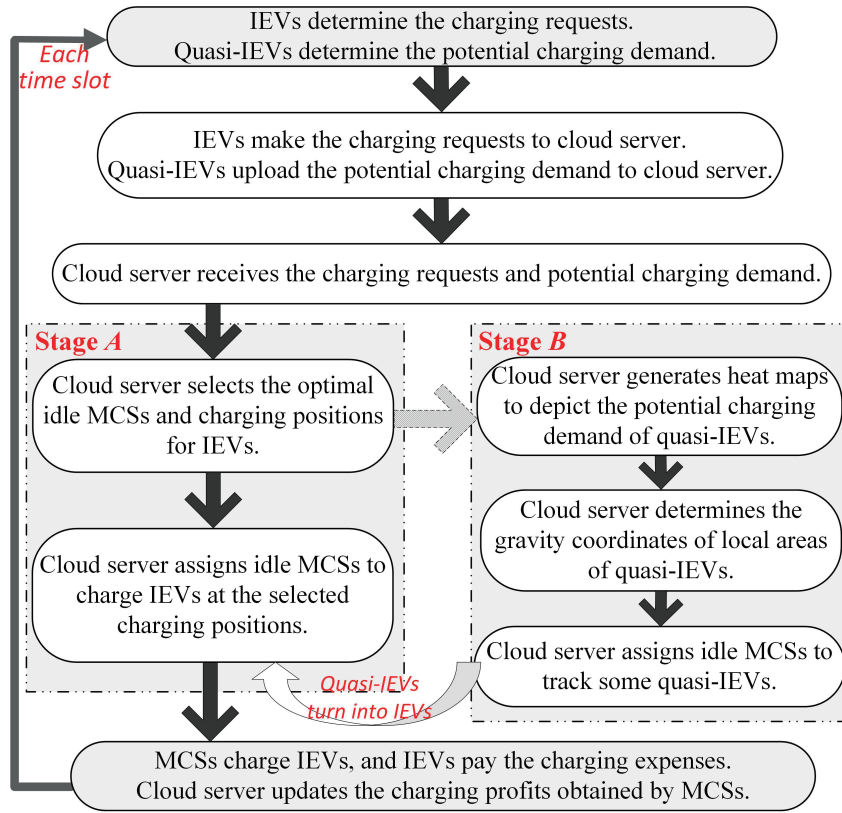


Fig. 6: The stages of PMASIM.

#### A. Stage A: Assignments of Idle MCSs for IEVs

The set of IEVs at the  $t$ -th time slot is denoted by  $\mathcal{E}_R^{(t)}$ . The set of idle MCSs at the  $t$ -th time slot is denoted by  $\mathcal{M}_I^{(t)}$ , and the set of MCSs having been assigned to charge IEVs at the previous time slots is denoted by  $\mathcal{M}_R^{(t)}$ .

Suppose an IEV  $v_i$  makes a charging request at the  $t$ -th time slot, and the charging request of  $v_i$  is expressed as:

$$\begin{aligned} \mathcal{CR}(v_i, t) = & \bigcup_{\tilde{p} \in \mathcal{I}} \{\tilde{p}, \Delta e(v_i, \tilde{p}), E_m(v_i, \tilde{p}), m_s(v_i)\}, \\ \text{s.t. } & e(v_i)^{(t)} \geq c \cdot |p(v_i)^{(t)} - \tilde{p}|. \end{aligned} \quad (8)$$

In (8),  $\mathcal{CR}(v_i, t)$  is comprised of several quadruples, where each quadruple  $\{\tilde{p}, \Delta e(v_i, \tilde{p}), E_m(v_i, \tilde{p}), m_s(v_i)\}$  has four components: (i) a potential charging position  $\tilde{p}$  determined by  $v_i$ , and  $\tilde{p}$  should satisfy the constraint  $e(v_i)^{(t)} \geq c \cdot |p(v_i)^{(t)} - \tilde{p}|$ , indicating that the residual electricity of  $v_i$  can support the movement from the current position  $p(v_i)^{(t)}$  to the charging position  $\tilde{p}$ ; (ii) the electricity of  $v_i$  to be charged at  $\tilde{p}$ ; (iii) the extra movement of  $v_i$  for being charged at  $\tilde{p}$ ; (iv) the moving speed of  $v_i$ .

After receiving the charging requests from the IEVs in  $\mathcal{E}_R^{(t)}$ , the cloud server selects the optimal idle MCSs and charging positions according to the objective of charging profit maximization. The optimal idle MCSs and charging

positions are selected by:

$$\arg \max \sum_{v_i \in \mathcal{E}_R^{(t)}, \psi_j \in \mathcal{M}_I^{(t)}} \left\{ \frac{\text{Exp}(v_i, \psi_j, \tilde{p}) - r_0 \cdot \Delta e(v_i, \tilde{p})}{-r_0 \cdot c \cdot |p(\psi_j)^{(t)} - \tilde{p}|} \right\}, \quad (9)$$

where  $\tilde{p} \in \mathcal{CR}(v_i, t)$ ,  $\text{delay}(v_i, \psi_j, \tilde{p}) \leq \tilde{D}$ .

In (9),  $\text{delay}(v_i, \psi_j, \tilde{p}) \leq \tilde{D}$  implies that the extra delay of  $v_i$  must be shorter than the allowable extra delay  $\tilde{D}$ . (9) implies that the optimal idle MCSs and charging positions are selected to maximize the charging profits of MCSs.

Especially, an idle MCS could be assigned to charge several IEVs simultaneously at the same charging position, and thus the charging profit of this MCS can be increased due to the reduction of charging cost. As illustrated in Fig. 7, three adjacent IEVs make the charging requests to the cloud server, and an idle MCS is assigned to charge them at the charging position  $\tilde{p}$  simultaneously.

#### B. Stage B: Assignments of Idle MCSs for Quasi-IEVs

Typically, MCSs are sparsely distributed on the road lattice, and thus the potential charging demand of quasi-IEVs should be uploaded to the cloud sever in advance for the charging preparations. Thus, the cloud server could assign idle MCSs to track quasi-IEVs for the potential charging in future. Otherwise, many quasi-IEVs could not be charged promptly, since they may be far away from idle MCSs when they turn into IEVs and make charging

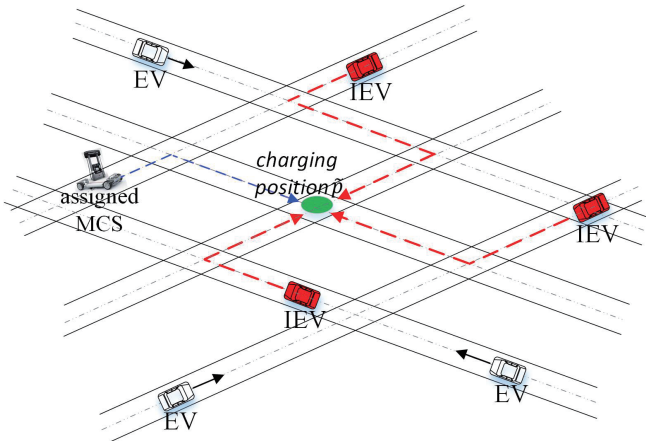


Fig. 7: An idle MCS is assigned to charge several IEVs.

requests.

**Stage B.1. Quasi-IEVs upload the potential charging demand to cloud server.** At the start of each time slot, each quasi-IEV uploads the potential charging demand to the cloud server. Similar to (8), the potential charging demand of a quasi-IEV  $v_i$  at the  $t$ -th time slot is expressed as a set of quadruples:

$$\begin{aligned} \mathcal{CD}(v_i, t) = \bigcup_{\hat{p} \in \mathcal{I}} \{\hat{p}, \Delta e(v_i, \hat{p}), E_m(v_i, \hat{p}), m_s(v_i)\}, \\ \text{s.t. } e(v_i)^{(t)} \geq c \cdot |p(v_i)^{(t)} - \hat{p}|, \end{aligned} \quad (10)$$

where  $\mathcal{E}_D^{(t)}$  denotes the set of quasi-IEVs at the  $t$ -th time slot. In a quadruple  $\{\hat{p}, \Delta e(v_i, \hat{p}), E_m(v_i, \hat{p}), m_s(v_i)\}$ , the tracking position  $\hat{p}$  is determined by  $v_i$ , and it is an available charging position supposing that  $v_i$  makes a charging request at the  $t$ -th time slot.

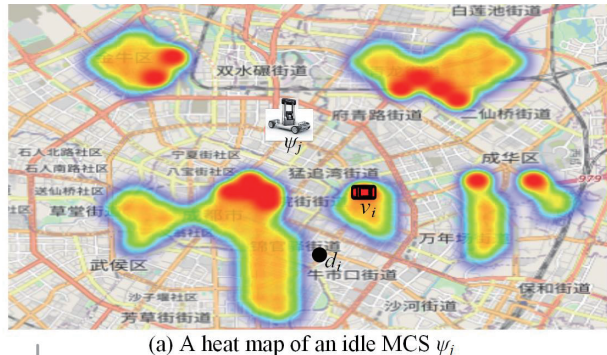
**Stage B.2. Cloud server generates the profit-maximizing heat maps for idle MCSs.** Upon receiving the potential charging demand from quasi-IEVs, the cloud server generates a profit-maximizing heat map for each idle MCS.

The profit-maximizing heat map of an idle MCS  $\psi_j$  (at the  $t$ -th time slot) is denoted by  $\Omega(\psi_j)^{(t)}$ , which is composed of several circular areas around the tracking positions.

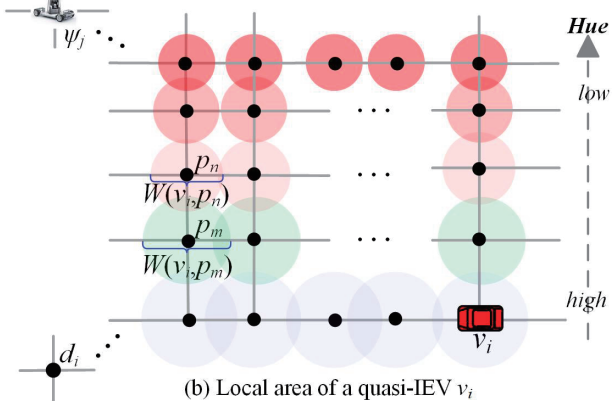
An example of the profit-maximizing heat map is provided in Fig. 8, where  $p_m$  and  $p_n$  denote two tracking positions. In Fig. 8(b), the diameter of the circular area  $C(v_i, p_m)$  around the tracking position  $p_m$  is given by:

$$W(v_i, p_m) = \begin{cases} 0, & \text{if } \text{delay}(v_i, \psi_j, p_m) > \tilde{D}, \\ W \cdot \left(1 - \frac{c \cdot E_m(v_i, \hat{p})}{\Delta e(v_i, \hat{p})}\right), & \text{otherwise,} \end{cases} \quad (11)$$

where  $W$  is a datum diameter, and the value of  $W(v_i, p_m)$  indicates the possibility of the quasi-IEV  $v_i$  passing through the tracking position  $p_m$ . In (11), the circular area where the quasi-IEV undertakes a shorter extra movement is with a larger diameter, due to the fact that quasi-IEVs prefer to undertake shorter extra movements.



(a) A heat map of an idle MCS  $\psi_j$



(b) Local area of a quasi-IEV  $v_i$

Fig. 8: A profit-maximizing heat map.

Besides, the hue of the circular area  $C(v_i, p_m)$  indicates the potential charging profit of  $\psi_j$  (obtained by charging  $v_i$  at the position  $p_m$ ), and the hue is calculated by:

$$H(v_i, \psi_j, p_m) = \left(1 - \frac{pf(v_i, \psi_j, p_m) - pf_{min}(\psi_j)}{pf_{max}(\psi_j) + 1 - pf_{min}(\psi_j)}\right) \times 240, \quad (12)$$

where "×240" enables the value of  $H(v_i, \psi_j, p_m)$  to fall into the hue range (0, 240) (from red to blue).  $pf_{min}(\psi_j)$  and  $pf_{max}(\psi_j)$  denote the minimum potential charging profit and the maximum potential charging profit respectively, and they are calculated by  $\psi_j$  according to the received potential charging demand of quasi-IEVs.

$pf(v_i, \psi_j, p_m)$  denotes the potential charging profit of  $\psi_j$  when  $\psi_j$  charges  $v_i$  at the position  $p_m$ , and  $pf(v_i, \psi_j, p_m)$  is expressed as:

$$\begin{aligned} pf(v_i, \psi_j, p_m) = & Exp(v_i, \psi_j, p_m) - r_0 \cdot \Delta e(v_i, p_m) \\ & - r_0 \cdot c \cdot |p(v_i)^{(t)} - p_m|. \end{aligned} \quad (13)$$

By the above mechanism, idle MCSs are directed to the areas where they could obtain larger charging profits in future.

**Stage B.3. Cloud server determines the gravity coordinates of local areas of quasi-IEVs.** In the profit-maximizing heat map  $\Omega(\psi_j)^{(t)}$ , the gravity coordinate of the local area

of  $v_i$  is denoted by  $g(v_i, \psi_j)^{(t)}$  and is determined by [19]:

$$g(v_i, \psi_j)^{(t)} = \left( \frac{\sum_{(x,y) \in \Omega(\psi_j)^{(t)}} x \cdot w(x,y)}{\sum_{(x,y) \in \Omega(\psi_j)^{(t)}} w(x,y)}, \frac{\sum_{(x,y) \in \Omega(\psi_j)^{(t)}} y \cdot w(x,y)}{\sum_{(x,y) \in \Omega(\psi_j)^{(t)}} w(x,y)} \right), \quad (14)$$

where  $(x, y)$  denotes a discrete coordinate, and  $(x, y)$  could be covered by several circular areas. We take a weight  $w(x, y)$  to measure the overlapped hue on  $(x, y)$ :  $w(x, y) = \sum_{(x,y) \in C(v_i, p_m)} \frac{1}{H(v_i, \psi_j, p_m)}$ ,  $\forall C(v_i, p_m) \in \Omega(\psi_j)^{(t)}$ .

Because the hue of a circular area indicates the potential charging profit of an idle MCS, the gravity coordinate calculated by (14) can be taken as the position where the idle MCS could charge some IEVs and approximatively obtain the maximum potential charging profit. However, the gravity coordinate could not be located on the road lattice, and thus the Profit-Maximization Tracking Position (PMTP) of  $v_i$  in  $\Omega(\psi_j)^{(t)}$  is selected as the available charging position on the road lattice which is closest to the gravity coordinate:

$$\begin{aligned} \mathcal{P}(v_i, \psi_j) &= \arg \min_{p_m \in \mathcal{CD}(v_i, t)} |g(v_i, \psi_j)^{(t)} - p_m|, \\ &\text{s.t. } \text{delay}(v_i, \psi_j, p_m) \leq \tilde{D}. \end{aligned} \quad (15)$$

**Stage B.4.** Cloud server assigns idle MCSs to track quasi-IEVs. Some idle MCSs are selected by cloud server to move towards the PMTPs of quasi-IEVs. The idle MCSs are selected by:

$$\arg \max_{v_i \in \mathcal{E}_D^{(t)}, \psi_j \in \mathcal{M}_I^{(t)}} \left\{ \begin{array}{l} \text{Exp}(v_i, \psi_j, \mathcal{P}(v_i, \psi_j)) \\ -r_0 \cdot \Delta e(v_i, \mathcal{P}(v_i, \psi_j)) \\ -r_0 \cdot c \cdot |p(\psi_j)^{(t)} - \mathcal{P}(v_i, \psi_j)| \end{array} \right\}. \quad (16)$$

In (16), the idle MCSs are selected to increase the potential charging profits as much as possible.

As a special case, some adjacent quasi-IEVs are allowed to share the same PMTP. For example, there are three quasi-IEVs  $v_1$ ,  $v_2$ , and  $v_3$ , as shown in Fig. 9. If  $v_1$ ,  $v_2$ , and  $v_3$  have some common tracking positions, and then a common tracking position  $\hat{p}$  is selected as the shared PMTP:

$$\begin{aligned} \mathcal{P}(v_1, v_2, v_3, \psi_j) &= \\ \arg \min \left\{ \begin{array}{l} |g(v_1, \psi_j)^{(t)} - \hat{p}| + |g(v_2, \psi_j)^{(t)} - \hat{p}| \\ + |g(v_3, \psi_j)^{(t)} - \hat{p}| \end{array} \right\}, \end{aligned} \quad (17)$$

where  $\hat{p} \in \mathcal{CD}(v_1, t) \cap \mathcal{CD}(v_2, t) \cap \mathcal{CD}(v_3, t)$ .

Then, an idle MCS can be assigned to move towards the shared PMTP to track  $v_1$ ,  $v_2$ , and  $v_3$  simultaneously.

## V. ANALYSIS OF PMASIM

### A. Complexity

TABLE II shows the communication complexity and computational complexity of the proposed PMASIM.

With regard to the communication complexity: (i) At each time slot, the charging requests (or potential charging demand) of IEVs (or quasi-IEVs) are uploaded to the cloud server, and the number of uploads is at most  $O(N)$ . (ii) The

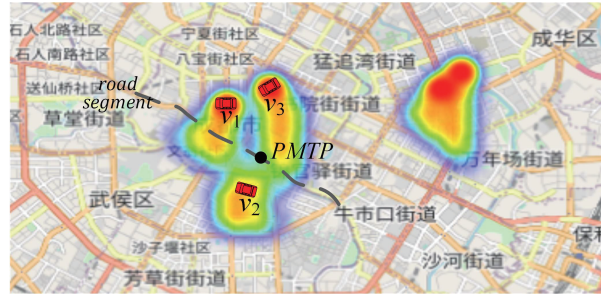


Fig. 9: Several adjacent quasi-IEVs share a PMTP.

current positions of idle MCSs are uploaded to the cloud server. The cloud server assigns idle MCSs to charge IEVs or track quasi-IEVs, and the number of communications for MCS assignments reaches  $O(M)$ .

With regard to the computational complexity: (i) In Stage A, the cloud server selects the optimal idle MCSs to charge IEVs, and the optimal assignments of idle MCSs are selected from  $N \cdot M$  available assignments. (ii) In Stage B.1, each quasi-IEV determines the potential charging demand, and the computational complexity of Stage B.1 is  $O(N)$  in the worst case. (iii) In Stage B.2, the cloud server generates a profit-maximizing heat map for each idle MCS, and a profit-maximizing heat map includes at most  $N$  circular areas, thereby the computation amount in Stage B.2 is  $O(N \cdot M)$ . (iv) In Stage B.3 and Stage B.4, the cloud server determines the gravity coordinates in profit-maximizing heat maps and selects the idle MCSs to track quasi-IEVs, and hence the computational complexity of Stage B.3 and Stage B.4 reaches  $O(N \cdot M)$ .

TABLE II: Complexity of PMASIM

Stage	Communication complexity	Computational complexity
A	$O(N + M)$	$O(N \cdot M)$
B.1	$O(N)$	$O(N)$
B.2	0	$O(N \cdot M)$
B.3	0	$O(N \cdot M)$
B.4	$O(M)$	$O(N \cdot M)$
Total	$O(N + M)$	$O(N \cdot M)$

Therefore, the communication complexity and computational complexity of PMASIM are written as  $O(N + M)$  and  $O(N \cdot M)$ , respectively.

### B. Expected Charging Profit of an MCS

Suppose the initial battery electricity of EVs follows a Gaussian distribution  $\mathcal{N}(\mu, \delta^2)$  [20], and then the expected probability of an EV exhausting its battery electricity before arriving at the destination is expressed as:

$$\mathbb{P}(c \cdot \mathbb{E}(\tilde{d}) > x > 0) = \Phi\left(\frac{c \cdot \mathbb{E}(\tilde{d}) - \mu}{\sigma}\right) - \Phi\left(\frac{-\mu}{\sigma}\right), \quad (18)$$

where  $x$  denotes the initial battery electricity of an EV, and  $\mathbb{E}(\tilde{d})$  denotes the expected distance from the departure position to the destination.

For an IEV  $v_i$ , the insufficient electricity  $\Delta e(v_i, \tilde{p})$  includes two parts: (i) the insufficient electricity for supporting the movement to the destination, written as  $c \cdot |s_i - d_i| - e(v_i)^{(0)}$ ; (ii) the electricity consumed for the extra movement, written as  $c \cdot E_m(v_i)$ .

$\left\lfloor \frac{x}{\gamma \cdot c} \right\rfloor$  denotes the longest extra movement of an IEV whose initial battery electricity is  $x$ . When EVs are deployed on a regular road lattice, the number of available charging positions (an IEV undertakes the extra movement distance of  $k$ ) is  $k + 1$ , and thus  $\frac{\left( \frac{x}{\gamma \cdot c} \right)}{\sum_{k=0}^{\left\lfloor \frac{x}{\gamma \cdot c} \right\rfloor} (\kappa + 1)}$  denotes the probability of an IEV undertaking the extra movement distance of  $k$ . Then, the expected extra movement of an IEV is expressed as:

$$\frac{1}{2} \cdot \int_{e_{min}}^{e_{max}} \frac{\exp\left(-\frac{(x-\mu)^2}{2\delta^2}\right)}{\sqrt{2\pi} \cdot \delta} \cdot \sum_{k=0}^{\left\lfloor \frac{x}{\gamma \cdot c} \right\rfloor} \frac{(k+1) \cdot k}{\sum_{\kappa=0}^{\left\lfloor \frac{x}{\gamma \cdot c} \right\rfloor} (\kappa+1)} dx, \quad (19)$$

where  $e_{max}$  and  $e_{min}$  denote the maximum battery electricity and the minimum battery electricity of EVs, respectively.

Thereby, the expected insufficient electricity of an IEV  $v_i$  is expressed as:

$$\begin{aligned} \mathbb{E}(\Delta e(v_i, \tilde{p})) &= \frac{\int_{e_{min}}^{c \cdot \mathbb{E}(\tilde{d})} \exp\left(-\frac{(x-\mu)^2}{2\delta^2}\right) \cdot (c \cdot \mathbb{E}(\tilde{d}) - x) dx}{\int_{e_{min}}^{c \cdot \mathbb{E}(\tilde{d})} \exp\left(-\frac{(x-\mu)^2}{2\delta^2}\right) dx} \\ &+ \frac{c}{2} \cdot \int_{e_{min}}^{e_{max}} \frac{\exp\left(-\frac{(x-\mu)^2}{2\delta^2}\right)}{\sqrt{2\pi} \cdot \delta} \cdot \sum_{k=0}^{\left\lfloor \frac{x}{\gamma \cdot c} \right\rfloor} \frac{(k+1) \cdot k}{\sum_{\kappa=0}^{\left\lfloor \frac{x}{\gamma \cdot c} \right\rfloor} (\kappa+1)} dx, \end{aligned} \quad (20)$$

where  $\frac{\int_{e_{min}}^{c \cdot \mathbb{E}(\tilde{d})} \exp\left(-\frac{(x-\mu)^2}{2\delta^2}\right) \cdot (c \cdot \mathbb{E}(\tilde{d}) - x) dx}{\int_{e_{min}}^{c \cdot \mathbb{E}(\tilde{d})} \exp\left(-\frac{(x-\mu)^2}{2\delta^2}\right) dx}$  denotes the expected insufficient electricity for supporting the movement to the destination.

Each quasi-IEV uploads the potential charging demand to the cloud server until it detects a low battery state. In the worst case, a quasi-IEV uploads the potential charging demand when it is with the initial battery electricity, i.e., it remains a quasi-IEV when the residual electricity falls into the range  $[\frac{\mu}{\gamma}, \mu]$ . Thus, the number of time slots for an idle MCS tracking a quasi-IEV is up to  $\frac{(\gamma-1) \cdot \mu}{\gamma \cdot c}$ , and the charging cost of an idle MCS is at most  $\frac{r_0 \cdot (\gamma-1) \cdot \mu}{\gamma}$ .

Moreover, due to the constraint of the allowable extra delay  $\tilde{D}$ , the maximum distance from the current position to the tracking position is written as  $\frac{\mu}{\gamma \cdot c} + \tilde{D} \cdot m_s$ , when each EV is assumed to move at the same moving speed  $m_s$ . Therefore, the expected charging profit of an MCS will be larger than the value of the following formula:

$$\begin{aligned} (r_e - r_0) \cdot \mathbb{E}(\Delta e(v_i, \tilde{p})) &- \frac{r_0 \cdot (\gamma-1) \cdot \mu}{\gamma} - r_0 \cdot c \cdot \left\{ \frac{\mu}{\gamma \cdot c} + \tilde{D} \cdot m_s \right\} \\ &= (r_e - r_0) \cdot \mathbb{E}(\Delta e(v_i, \tilde{p})) - r_0 \cdot \mu - r_0 \cdot c \cdot \tilde{D} \cdot m_s, \end{aligned} \quad (21)$$

which indicates that a larger  $\mu$  or  $\tilde{D}$  makes the movements of quasi-IEVs more uncertain, and thereby could reduce the charging profits of MCSs. To this end, in PMASIM the idle MCSs are preferentially assigned to charge IEVs

rather than to track quasi-IEVs, especially when the number of idle MCSs is very small.

## VI. PERFORMANCE EVALUATIONS

In this section, we provide some performance evaluations on our proposed PMASIM. The simulations are conducted on a taxi dataset provided by Didi Corporation [21]. This dataset contains the GPS trajectories of more than 10,000 taxis during the period from Oct. 1, 2018 to Oct. 31, 2018 in Chengdu city, China. Each GPS trajectory is represented by a sequence of timestamps, latitudes, longitudes, and taxi ID. Note that the passengers of taxis and the drivers of EVs have similar travel intentions in their daily lives. Thus, this dataset is adopted for our simulations, and we use these taxi trajectories to simulate the movements of EVs.

Some examples of profit-maximizing heat maps selected from different time intervals are shown in Fig. 10, which indicates that the charging demand of EVs during the time interval from 4:00 AM to 8:00 AM is the smallest, and that during the time interval from 16:00 PM to 24:00 PM is the highest. The main parameter settings are shown in TABLE III.

TABLE III: Simulation parameters

Parameter	Description	Value
$N$	Number of EVs	500
$M$	Number of MCSs	18
$t_s$	Length of each time slot	60 s
$T$	Number of time slots in an observation period	1440
$\xi$	Charging power of MCSs	240 kw
$\tilde{D}$	Allowable extra delay	450 s
$m_s$	Moving speed of each EV or each MCS	11.1 m/s
$e(v_i)^{(0)}$	Battery capacity of each EV	90 kwh
$\mu_r$	Average residual electricity of IEVs	12.5 kwh
$\delta_r$	Standard deviation of residual electricity of IEVs	5 kwh
$c$	Electricity consumption for moving through a unit distance	0.5 kwh/km
$r_e$	Unit price of electricity transferred from MCSs to IEVs	2.4 /kwh
$r_0$	Unit price of electricity purchased from power grid	1.0 /kwh
$\gamma$	Low battery parameter for an IEV making a charging request	18
$\gamma_d$	Low battery parameter for a quasi-IEV uploading a potential charging demand	9
$W$	Datum diameter	500 m

### A. Charging Experience of IEVs

The proportion of charged IEVs and the average waiting time of IEVs can measure the charging experience of IEVs.

Fig. 11 illustrates the impacts of  $\mu_r$ ,  $\delta_r$ ,  $\tilde{D}$ ,  $N$ , and  $M$  on the proportion of charged IEVs. In Fig. 11(a), the proportion of charged IEVs is increased with the increase of  $\mu_r$  or  $\tilde{D}$ . This is because the IEVs with more residual electricity or restricted by a longer allowable extra delay could have more available MCSs, and hence they are more likely to be charged by MCSs.

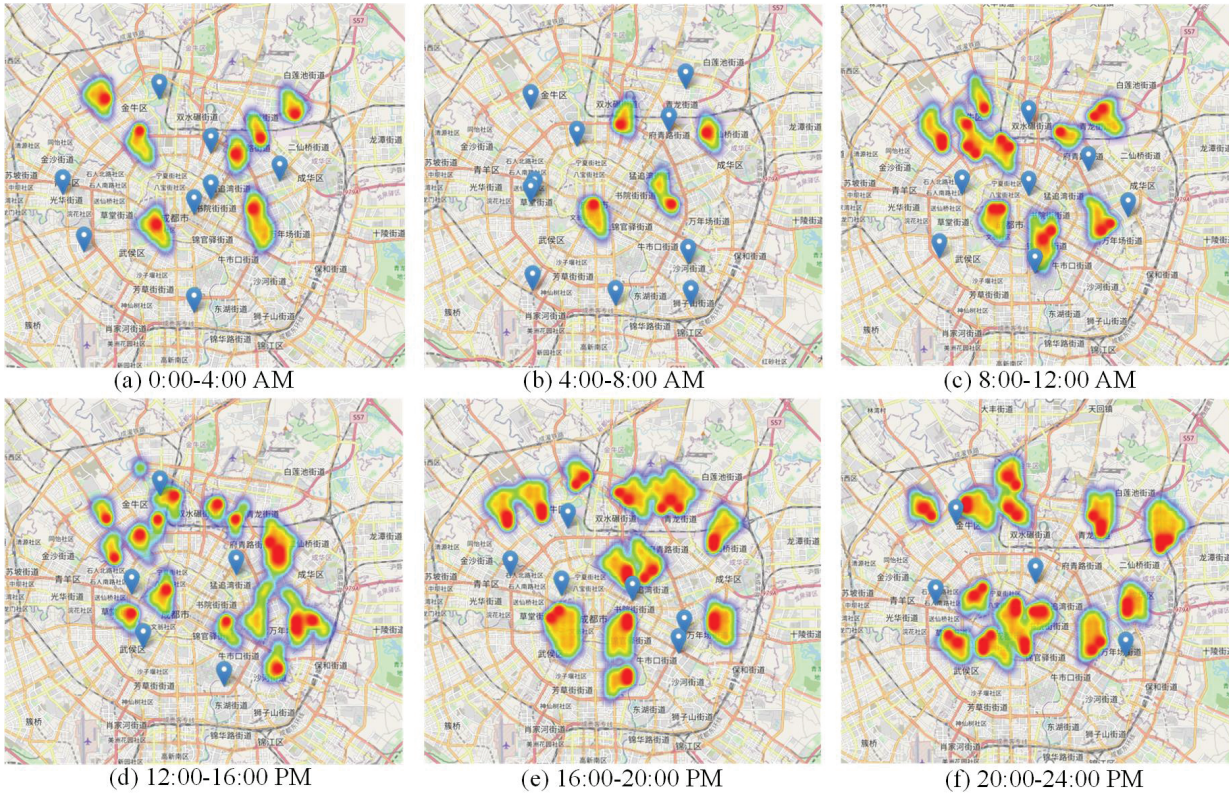


Fig. 10: Some examples of profit-maximizing heat maps selected from different time intervals.

In Fig. 11(b) and Fig. 11(c), the proportion of charged IEVs is decreased with the increase of  $\delta_r$  or  $N$ , since more IEVs exist and compete for the charging services of MCSs. Thus, the proportion of uncharged IEVs becomes larger. Besides, the proportion of charged IEVs is evidently increased when more MCSs are deployed on the road lattice, as illustrated in Fig. 11(c).

Fig. 12 shows that the average waiting time of IEVs is shortened with the increase of  $M$ , which is attributed to the fact that IEVs can be charged more conveniently when more MCSs are provided. Note that the average waiting time of IEVs is nearly independent of  $N$ . This is because when more IEVs exist and are distributed more densely, some IEVs can be simultaneously charged (as depicted in Fig. 7), while more IEVs also intensify the competition of charging services (e.g., some IEVs are charged after MCSs have charged other IEVs). This phenomenon indicates that PMASIM has a favorable scalability in terms of the average waiting time of IEVs, due to the mechanism adopted in PMASIM that an idle MCS is allowed to charge several IEVs or track several quasi-IEVs simultaneously.

#### B. Average Profit of MCSs and Average Movement Distance of MCSs

The charging profits of MCSs are related to the number of charged IEVs, i.e., a larger number of charged IEVs typically gives rise to larger charging profits of MCSs. Fig. 13(a) suggests that the average profit of MCSs is increased with the increase of EVs' number, due to the

fact that larger charging profits are obtained by MCSs when there are more IEVs to be charged by MCSs.

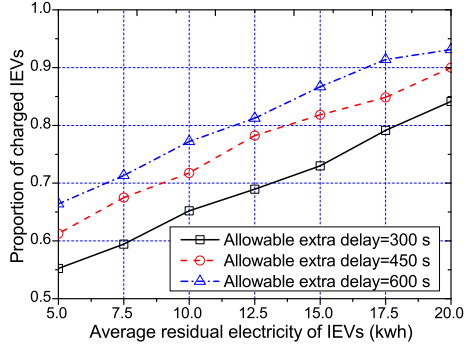
Besides, the curve with a larger  $M$  is lower than that with a smaller one. This is because the charging services and charging profits are shared by all MCSs, and the average profit of MCSs is reduced when more MCSs are deployed on the road lattice. However, with more MCSs, IEVs can be charged more promptly, and the charging experience of IEVs is certainly improved.

With the increase of  $N$  or the decrease of  $M$ , an MCS could charge more IEVs simultaneously, and a tradeoff should be made among these IEVs regarding the selection of the charging position. Thus, the average movement distance of MCSs after being requested is increased, as shown in Fig. 13(b).

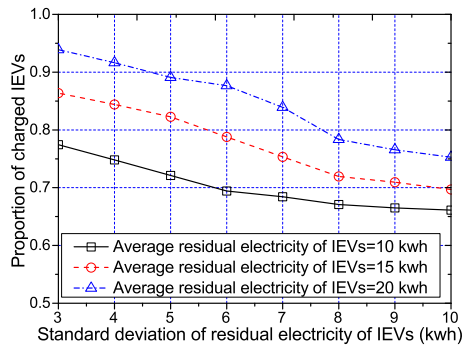
#### C. Average Expense of IEVs

In Fig. 14(a), the average expense of IEVs is increased with the increase of EVs' number, and the reason is that longer extra movements are undertaken by the charged IEVs when more IEVs compete for the charging services of MCSs. In contrast, IEVs are more likely to be charged when there are more MCSs (a larger  $M$ ), and hence the average expense of IEVs is decreased.

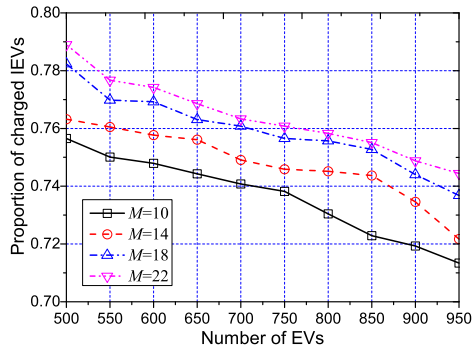
Fig. 14(b) shows that the average expense of IEVs is reduced when the average residual electricity of IEVs becomes larger, because less electricity is required by IEVs. Besides, the average expense of IEVs is slowly increased



(a) Proportion of charged IEVs vs.  $\mu_r$ , and  $\tilde{D}$



(b) Proportion of charged IEVs vs.  $\delta_r$ , and  $\mu_r$



(c) Proportion of charged IEVs vs.  $N$ , and  $M$

Fig. 11: Proportion of charged IEVs.

with the increase of  $\delta_r$ , since a larger  $\delta_r$  implies that the insufficient electricity of IEVs becomes larger.

#### D. Average Charging Cost of MCSs

As shown in Fig. 15(a), the average charging cost of MCSs is reduced with the increase of  $\mu_r$  or the decrease of  $\tilde{D}$ . A larger  $\mu_r$  implies that IEVs have more residual electricity to undertake longer extra movements, and thus reduce the movements of MCSs. Under a larger  $\tilde{D}$ , more IEVs could stay and wait for the arrivals of MCSs, which increases the movements of MCSs.

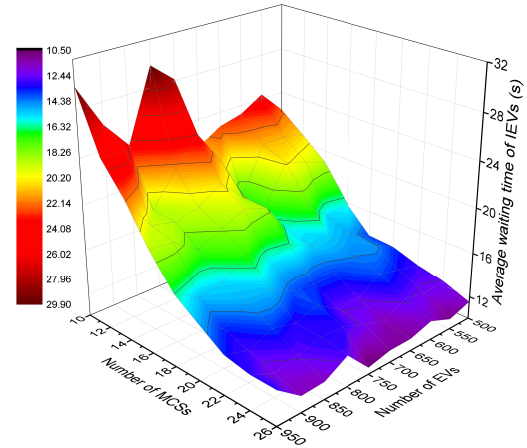
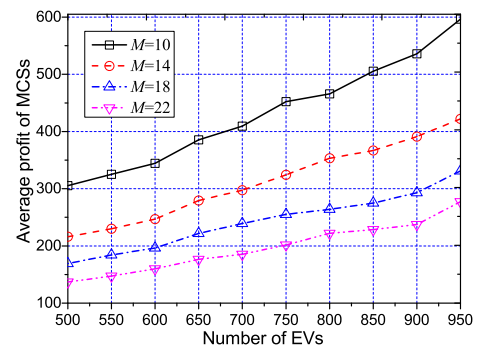
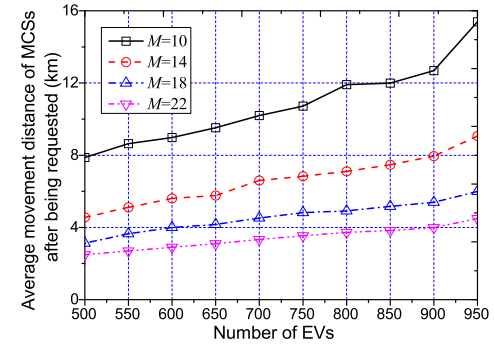


Fig. 12: Average waiting time of IEVs.



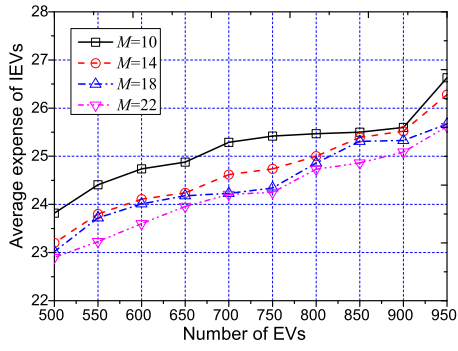
(a) Average profit of MCSs



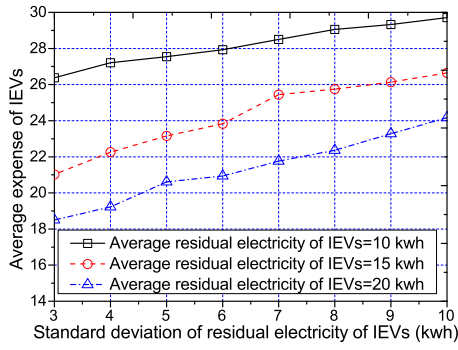
(b) Average movement distance of MCSs after being requested

Fig. 13: Average profit of MCSs, and average movement distance of MCSs after being requested.

Moreover, Fig. 15(b) indicates that smaller charging cost is produced by MCSs when fewer EVs or more MCSs are deployed, because the movements of MCSs can be reduced when better idle MCSs are selected to charge IEVs or track quasi-IEVs.



(a) Average expense of IEVs vs.  $N$ , and  $M$



(b) Average expense of IEVs vs.  $\delta_r$ , and  $\mu_r$

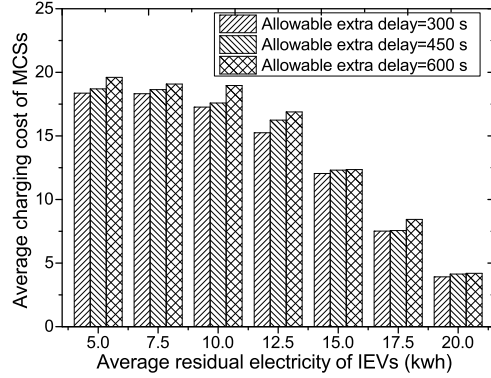
Fig. 14: Average expense of IEVs.

#### E. Strategy Comparisons

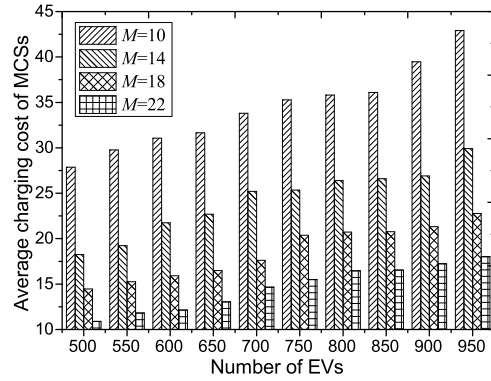
To further verify the merits of PMASIM, we compare PMASIM with some related strategies, such as stationary strategy (idle MCSs remain stationary), random walk strategy (idle MCSs move randomly), CWSH strategy (Clarke and Wright Saving's Heuristics [12]), and RBA [6]. These strategies are compared in terms of proportion of charged IEVs, average waiting time of IEVs, average profit of MCSs, average expense of IEVs, and average charging cost of MCSs. The simulation results are given in Fig. 16, Fig. 17, and Fig. 18.

Fig. 16 indicates that PMASIM achieves preferable results in terms of proportion of charged IEVs and average waiting time of IEVs. The reason is that PMASIM evaluates the potential charging profits of idle MCSs and properly assigns idle MCSs to track quasi-IEVs, and thus quasi-IEVs could be promptly charged after they turn into IEVs, which enhances the proportion of charged IEVs and shortens the waiting time of IEVs. Accordingly, PMASIM yields the shortest average movement distance of MCSs (Fig. 17(a)).

In particular, RBA achieves the shortest average waiting time of IEVs in Fig. 16(b), because RBA selects the charging positions where IEVs could spend the shortest time on being charged, and the assigned MCSs always arrive at the charging positions prior to IEVs. However, the average movement distance of MCSs obtained by RBA is much



(a) Average charging cost of MCSs vs.  $\mu_r$ , and  $\tilde{D}$



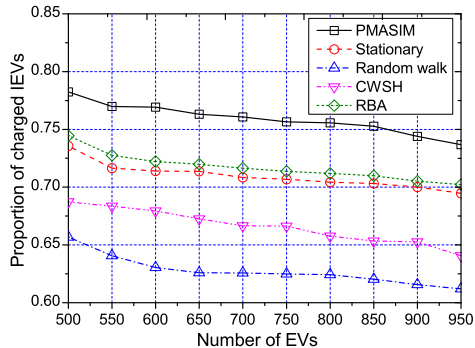
(b) Average charging cost of MCSs vs.  $N$ , and  $M$

Fig. 15: Average charging cost of MCSs.

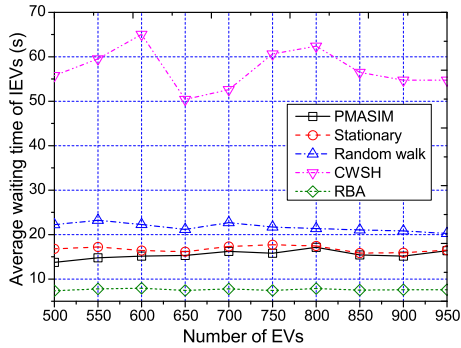
larger than that of PMASIM (Fig. 17(a)), due to the fact that IEVs are far away from idle MCSs when the assignments of idle MCSs for quasi-IEVs are not considered.

In real MCS charging scenarios, a tradeoff among the charging profits of MCSs, charging expenses of IEVs, and charging cost of MCSs should be made. In Fig. 17(b), the average profit obtained by CWSH is slightly larger than that obtained by PMASIM, since the extra movements of IEVs in CWSH are much longer than those in PMASIM, and thereby MCSs earn more profits through charging more electricity to IEVs. However, the charging expenses of IEVs obtained by CWSH are much larger than others (Fig. 18(a)), which is unbearable to EV owners. Essentially, CWSH increases the charging profits of MCSs by increasing the charging expenses of IEVs, rather than promoting the charging efficiency of MCSs.

The random walk strategy yields the smallest average profit of MCSs and the largest average charging cost of MCSs, indicating that the random walks of idle MCSs worsen the charging efficiency significantly. On the contrary, with regard to the stationary strategy, the average expense of IEVs (Fig. 18(a)) and the average charging cost of MCSs (Fig. 18(b)) are the smallest among the four strategies,



(a) Proportion of charged IEVs



(b) Average waiting time of IEVs

Fig. 16: Comparisons of proportion of charged IEVs, and average waiting time of IEVs.

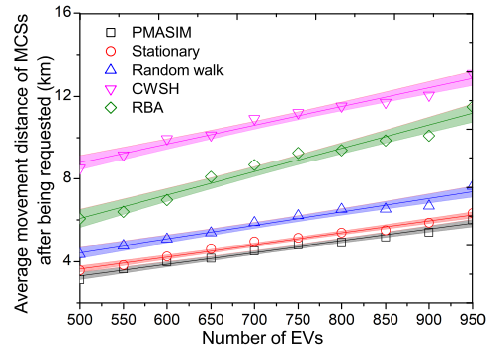
while the average profit of MCSs is not preferable.

The above results suggest that our proposed PMASIM can make a preferable tradeoff among the charging profits of MCSs, charging expenses of IEVs, and charging cost of MCSs.

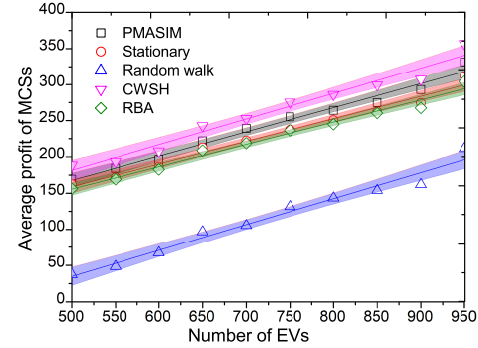
## VII. CONCLUSION

We have studied the problem of MCS assignments in an IoEV, and the Profit-Maximizing Assignment Strategy of Idle MCSs (PMASIM) has been proposed. In PMASIM, the profit-maximizing heat maps are applied to depict the potential charging demand of quasi-IEVs and evaluate the potential charging profits of idle MCSs. The idle MCSs are assigned to charge IEVs at selected charging positions, or track quasi-IEVs according to the profit-maximizing heat maps. Consequently, PMASIM increases the charging profits of MCSs and enhances the proportion of charged IEVs effectively.

Moreover, there are some practical issues related to the problem of MCS assignments: (i) The electric capacity of MCSs is limited as well, and some MCSs could be temporarily offline due to the lack of electric energy. These MCSs should be charged by the power grid, and therefore the route schedules of MCSs should take into account both charging IEVs and being charged by the power grid.



(a) Average movement distance of MCSs after being requested



(b) Average profit of MCSs

Fig. 17: Comparisons of average movement distance of MCSs after being requested, and average profit of MCSs (confidence interval=0.95).

(ii) This work mainly focuses on the assignments of MCSs, and FCSs are not considered in the model and the proposed strategy. IoEV with both FCSs and MCSs is more practical. Specially, these FCSs and MCSs could have different moving speed, charging capacity, and number of charging interfaces. How to improve the charging efficiency by properly utilizing the heterogeneous charging facilities remains another important issue.

## ACKNOWLEDGMENTS

This research is supported by National Natural Science Foundation of China under Grant Nos. 62272237, 61872193.

## REFERENCES

- [1] I. S. Bayram, G. Michailidis, M. Devetsikiotis, et al, "Electric power allocation in a network of fast charging stations," *IEEE Journal on Selected Areas in Communications*, vol. 31, no. 7, pp. 1235–1246, 2013.
- [2] E. Akhavan-Rezai, M. F. Shaaban, E. F. El-Saadany, et al, "Online intelligent demand management of plug-in electric vehicles in future smart parking lots," *IEEE Systems Journal*, vol. 10, no. 2, pp. 483–494, 2016.
- [3] C. C. Lin, D. J. Deng, C. C. Kuo, et al, "Optimal charging control of energy storage and electric vehicle of an individual in the Internet of energy with energy trading," *IEEE Transactions on Industrial Informatics*, vol. 14, no. 6, pp. 2570–2578, 2018.

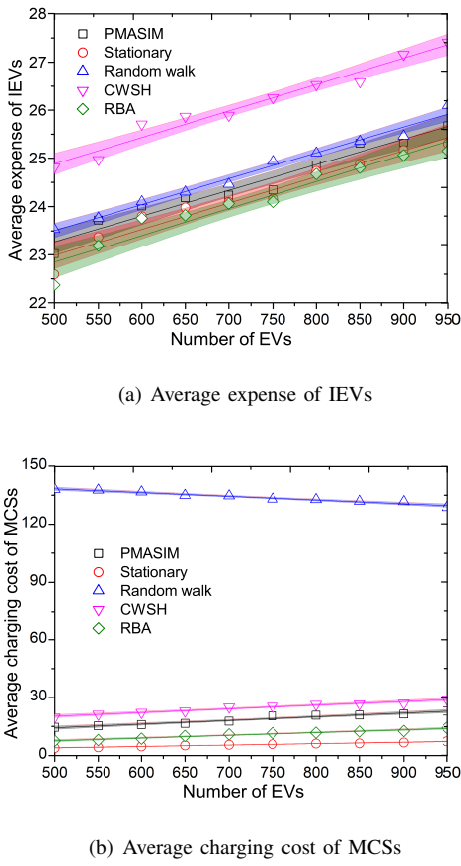


Fig. 18: Comparisons of average expense of IEVs, and average charging cost of MCSs (confidence interval=0.95).

- [4] H. Zhang, B. Jin, J. Li, *et al*, “Optimized scheduling for urban-scale mobile charging vehicle,” *2nd World Symposium on Communication Engineering (WSCE)*, Nagoya, Japan, 2019.
- [5] H. Chen, Z. Su, Y. Hui, *et al*, “Dynamic charging optimization for mobile charging stations in Internet of Things,” *IEEE Access*, vol. 6, pp. 53509–53520, 2018.
- [6] X. Zhang, Y. Cao, L. Peng, *et al*, “Mobile charging as a service: a reservation-based approach,” *IEEE Transactions on Automation Science and Engineering*, vol. 17, no. 4, pp. 1976–1988, 2020.
- [7] D. Liu, Z. Xu, Y. Zhou, *et al*, “Heat map visualisation of fire incidents based on transformed sigmoid risk model,” *Fire Safety Journal*, vol. 109, 2019.
- [8] F. Lateef, M. Kas, and Y. Ruichek, “Saliency heat-map as visual attention for autonomous driving using generative adversarial network (GAN),” *IEEE Transactions on Intelligent Transportation Systems*, vol. 23, no. 6, pp. 5360–5373, 2022.
- [9] M. Wang, H. Liang, R. Deng, *et al*, “Mobility-aware coordinated charging for electric vehicles in VANET-enhanced smart grid,” *IEEE Journal on Selected Areas in Communications*, vol. 32, no. 7, pp. 1344–1360, 2014.
- [10] P. Liu, C. Wang, J. Hu, *et al*, “Joint route selection and charging discharging scheduling of EVs in V2G energy network,” *IEEE Transactions on Vehicular Technology*, vol. 69, no. 10, pp. 10630–10641, 2020.
- [11] V. Chauhan, and A. Gupta, “Scheduling mobile charging stations for electric vehicle charging,” *14th International Conference on Wireless and Mobile Computing, Networking and Communications (WiMob)*, Limassol, Cyprus, 2018.
- [12] U. Qureshi, A. Ghosh, and B. K. Panigrahi, “Scheduling and routing of mobile charging stations to charge electric vehicles in a smart-city,” *IEEE 17th India Council International Conference (INDICON)*, New Delhi, India, 2020.
- [13] Y. Jin, J. Xu, S. Wu, *et al*, “Enabling the wireless charging via bus

network: route scheduling for electric vehicles,” *IEEE Transactions on Intelligent Transportation Systems*, vol. 22, no. 3, pp. 1827–1839, 2021.

- [14] L. Liu, X. Qi, Z. Xi, *et al*, “Charging-expense minimization through assignment rescheduling of movable charging stations in electric vehicle networks,” *IEEE Transactions on Intelligent Transportation Systems*, vol. 23, no. 10, pp. 17212–17223, 2022.
- [15] L. Liu, Z. Xi, K. Zhu, *et al*, “Mobile charging station placements in Internet of Electric Vehicles: A federated learning approach,” *IEEE Transactions on Intelligent Transportation Systems*, vol. 23, no. 12, pp. 24561–24577, 2022.
- [16] Q. Wang, J. Wang, C. Lei, *et al*, “Short-term planning model for distribution network restructuring based on heat maps,” *IET Generation, Transmission & Distribution*, vol. 12, no. 14, pp. 3569–3577, 2018.
- [17] C. Li, Q. Wang, C. Lei, *et al*, “A short-term planning model for restructuring distribution network based on heat maps,” *2018 IEEE Power & Energy Society General Meeting (PESGM)*, Portland, USA, 2018.
- [18] R. Netek, T. Pour, and R. Slezakova, “Implementation of heat maps in geographical information system – exploratory study on traffic accident data,” *Open Geosciences*, vol. 10, no. 1, 2018.
- [19] H. C. V. Assen, M. Egmont-Petersen, and J. H. C. Reiber, “Accurate object localization in gray level images using the center of gravity measure: accuracy versus precision,” *IEEE Transactions on Image Processing*, vol. 11, no. 12, pp. 1379–1384, 2002.
- [20] R. R. Richardson, M. A. Osborne, and D. A. Howey, “Gaussian process regression for forecasting battery state of health,” *Journal of Power Sources*, vol. 357, pp. 209–219, 2017.
- [21] Didi Corporation, “GAIA open dataset,” <http://outreach.didichuxing.com/research/opendata>, 2020.

#### AUTHOR BIOGRAPHY

**Linfeng Liu** received the B. S. and Ph. D. degrees in computer science from the Southeast University, Nanjing, China, in 2003 and 2008, respectively. At present, he is a Professor in the School of Computer Science and Technology, Nanjing University of Posts and Telecommunications, China. His main research interests include the areas of vehicular ad hoc networks, wireless sensor networks and multi-hop mobile wireless networks. He has published more than 80 peer-reviewed papers in some technical journals or conference proceedings, such as IEEE TMC, IEEE TPDS, IEEE TIFS, IEEE TSC, ACM TAAS, ACM TOIT, IEEE TVT, IEEE IoTJ, Computer Networks, Elsevier JPDC. He has served as the TPC member of Globecom, ICONIP, VTC, WCSP.

**Houqian Zhang** received the B. S. degree in computer science from the Wuhan University of Science and Technology in 2020. At present, he is a master student of Nanjing University of Posts and Telecommunications. His current research interest includes the areas of mobile opportunistic networks and electric vehicular networks.

**Jia Xu** received the Ph. D. Degree in School of Computer Science and Engineering from Nanjing University of Science and Technology, Jiangsu, China, in 2010. He is currently a professor in Jiangsu Key Laboratory of Big Data Security and Intelligent Processing at Nanjing University of Posts and Telecommunications. His main research interests include crowdsourcing, edge computing and wireless sensor networks. Prof. Xu has served as the PC Co-Chair of SciSec 2019, Organizing Chair of ISKE 2017, TPC member of Globecom, ICC,

MASS, ICNC, EDGE.

**Ping Wang** received her Bachelor and Master degrees from Huazhong University of Science and Technology, in 1994 and 1997, respectively, and her PhD degree from the University of Waterloo, Canada, in 2008, all in electrical and computer engineering. She joined York University as an Associate Professor in August 2018. Prior to that, she worked with Nanyang Technological University, Singapore, from 2008 to July 2018. Her research interests are mainly in wireless communication networks, cloud computing and the Internet of Things. Her scholarly works have been widely disseminated through top-ranked IEEE journals/conferences and received the Best Paper Awards from IEEE Wireless Communications and Networking Conference (WCNC) in 2012 and 2020, from IEEE Communication Society: Green Communications & Computing Technical Committee in 2018, and from IEEE International Conference on Communications (ICC) in 2007. She is a Fellow of the IEEE and a Distinguished Lecturer of the IEEE Vehicular Technology Society.